

ANTI-JAMMING GPS RECEIVERS BASED ON BILINEAR SIGNAL DISTRIBUTIONS

Yimin Zhang[†], Moeness G. Amin[†], and Alan R. Lindsey[‡]

[†] Department of Electrical and Computer Engineering,
Villanova University, Villanova, PA 19085
E-mail: {zhang,moeness}@ece.villanova.edu

[‡] Air Force Research Laboratory,
525 Brooks Road, Rome, NY 13441
E-mail: alan.lindsey@rl.af.mil

ABSTRACT

In this paper, we propose a nonstationary jammer suppression technique for GPS receivers. This technique is based on using the time-frequency distributions (TFDs) to define the jammer time-frequency (t-f) signature. A mask can be constructed and applied such that the masked t-f region captures the jammer energy, but leaves out most of the GPS signals. The jammer signals are synthesized from the masked TFDs and removed from the received signal by orthogonal projection. A method for determining an appropriate mask is discussed. We extend the proposed jammer excision method to multi-antenna GPS receivers.

1. INTRODUCTION

The ever-increasing reliance on GPS for navigation and guidance has created a growing awareness of the need for adequate protection against both unintentional and intentional jammers. Designers of military as well as commercial communication systems have, through the years, developed numerous anti-jamming techniques to counter these threats. On the other hand, as these techniques become effective for interference removal and mitigation, jammers themselves have become smarter and more sophisticated, and generate signals, which are difficult to combat. In this sense, non-stationary jamming signals are difficult to mitigate using conventional techniques.

Thus far, the authors have proposed orthogonal projection techniques to suppress instantaneously narrowband jammer signals. These techniques are based on the temporal or spatio-temporal signatures of the jammer signals [1, 2]. Only instantaneously narrowband frequency modulated (FM) jammers have been considered. The jammer subspace was derived based on the estimation of its instantaneous frequency (IF).

In this paper, we propose the use of time-frequency distribution (TFD) signal synthesis methods to estimate the jammer subspace. By using signal synthesis techniques [3],

This work is supported by the Air Force Research Laboratory, Grant no. F30602-00-1-0515.

we can estimate the subspace of a general class of nonstationary jammers, provided that they are localizable in the time-frequency (t-f) domain. Compared with the t-f subspace method [4], the proposed method confines the jammer to a single-dimensional subspace and, as such, reduces the GPS signal distortion due to projections.

The received signal is a mixture of the jammers, the additive noise, and the desired GPS signals. Therefore, in order to synthesize the jammer components, it is important to construct a mask in the t-f domain such that the masked t-f region contains most of the jammer energy and minimal GPS signal power. In this paper, a simple method that applies a threshold value to construct an appropriate t-f mask for the underlying application is applied.

Finally, we extend the proposed method to multi-antenna GPS receivers. It is shown that the use of multiple antennas can improve the performance in two ways: (a) The array averaged TFDs can be exploited to reduce the effect of crossterms as well as noise. (b) The use of array sensors extends the signal dimensions and, therefore, can reduce the signal distortion due to orthogonal projection.

2. SIGNAL MODEL

In the GPS system, the navigation signal is BPSK modulated, and the symbol rate is $1/T_s = 50$ symbols/sec. In this paper, we consider the coarse acquisition (C/A) code. The input signal-to-noise ratio (SNR) of a GPS signal is usually in the range of -14 dB to -20 dB.

The BPSK-modulated DS/SS signal, in the discrete time form sampled at the chip rate, can be expressed as

$$p(t) = \sum_n I_n c(t - nL_0) \quad (1)$$

where $I_n \in \{-1, 1\}$ represents the binary information sequence, and $c(t)$ is the spreading code with length L_0 .

We first consider the single antenna case. The signal

waveform is expressed as

$$x(t) = p(t) + \sum_{v=1}^J j_v(t) + w(t) \quad (2)$$

where $p(t)$ is the GPS signal, $j_v(t)$ is the v th jammer ($v = 1, \dots, J$), and $w(t)$ is the additive noise. The noise components is modeled as zero-mean, independent and identically distributed (i.i.d.) Gaussian random vectors with autocovariance $\sigma\mathbf{I}$, where \mathbf{I} is the identity matrix. Also, the noise is assumed independent from the GPS signal and the jammers.

By storing L symbols (we consider L as a general positive integer and is not necessarily the same as L_0), the above equation can be written in the vector form

$$\mathbf{x} = \mathbf{p} + \sum_{v=1}^J \mathbf{j}_v + \mathbf{w} \quad (3)$$

where $\mathbf{x} = [x(1) \ x(2) \ \dots \ x(L)]$, $\mathbf{p} = [p(1) \ p(2) \ \dots \ p(L)]$, $\mathbf{j}_v = [j_v(1) \ j_v(2) \ \dots \ j_v(L)]$, and $\mathbf{w} = [w(1) \ w(2) \ \dots \ w(L)]$. It is noted that the vector \mathbf{p} is real, whereas all other vectors in the above equation have complex entries.

3. JAMMER SYNTHESIS BASED ON TIME-FREQUENCY DISTRIBUTIONS

3.1. Signal Synthesis Based on Extended Discrete-Time Wigner Distribution

The signal synthesis techniques based on Wigner-Ville distributions can be found in [3, 5]. In this paper, the method of extended discrete-time Wigner distribution (EDTWD), introduced in [6], is applied. The advantage of using the EDTWD in signal synthesis lies in the fact that it does not require *a priori* knowledge of the source waveform, and thereby avoids the problem of matching the two “uncoupled” even-indexed and odd-indexed vectors.

The overall procedure of EDTWD-based signal synthesis is summarized in the following steps.

- Given the received data of $x(t)$, compute the EDTWD

$$W_{xx}(t, f) = \sum_{k:t+\frac{k}{2} \in Z} x(t + \frac{k}{2}) x^*(t - \frac{k}{2}) e^{-j2\pi kf}, \quad (4)$$

$$t = 0, \pm\frac{1}{2}, \pm 1, \dots,$$

where the superscript * denotes complex conjugation.

- Take the inverse Fourier transform of $W_{xx}(t, f)$

$$p(t, \tau) = \int W_{xx}(t, f) e^{j2\pi\tau f} df. \quad (5)$$

- Construct the matrix $\mathbf{Q} = [q_{i,j}]$ with

$$q_{i,j} = p \left(\frac{i+j}{2}, i-j \right). \quad (6)$$

- Take the Hermitian component \mathbf{Q}_H of \mathbf{Q}

$$\mathbf{Q}_H = \frac{1}{2} [\mathbf{Q} + \mathbf{Q}^H], \quad (7)$$

where the superscript H denotes transpose conjugation.

5. Apply eigen-decomposition to the matrix \mathbf{Q}_H and obtain the maximum eigenvalue λ_{\max} and the associated eigenvector \mathbf{u} . The synthesis signal is given by

$$\hat{x} = e^{j\phi} \sqrt{\lambda_{\max}} \mathbf{u}, \quad (8)$$

where ϕ is an unknown value representing the phase ambiguity.

3.2. Time-Frequency Masking

In the underlying problem, we synthesize the jammer from the TFD of a mixture of the jammer signals and the GPS signals along with the additive noise. Assuming the jammer has a distinct t-f profile, then its waveform can be extracted by applying an appropriate t-f mask.

From (2) and (4), the EDTWD for the single jammer case is

$$\begin{aligned} W_{xx}(t, f) &= W_{pp}(t, f) + W_{jj}(t, f) + W_{ww}(t, f) \\ &\quad + W_{pj}(t, f) + W_{pw}(t, f) + W_{jp}(t, f) \\ &\quad + W_{jw}(t, f) + W_{wp}(t, f) + W_{wj}(t, f) \\ &= W_{pp}(t, f) + W_{jj}(t, f) + W_{ww}(t, f) \\ &\quad + 2\text{Re}(W_{pj}(t, f) + W_{pw}(t, f) + W_{jw}(t, f)), \end{aligned} \quad (9)$$

where $\text{Re}(\cdot)$ denotes the real part operator. In (9), the first three terms are the autoterms of the GPS signal, the jammer, and the noise, and the other terms are their respective crossterms. The crossterm EDTWD between two variables $x(t)$ and $y(t)$ is defined as

$$W_{xy}(t, f) = \sum_{k:t+\frac{k}{2} \in Z} x(t + \frac{k}{2}) y^*(t - \frac{k}{2}) e^{-j2\pi kf} = W_{yx}^*(t, f). \quad (10)$$

With the exception of the autoterm $W_{jj}(t, f)$, all other auto- and cross-terms, including the autoterm of the GPS signal $W_{pp}(t, f)$, spread over the entire t-f domain. Therefore, to synthesize the jammer signal, exclusive from the GPS signal, one need to only mask out the autoterm of the jammer. Denote $M(t, f)$ as an appropriate t-f mask. Then, the masked TFD is expressed as

$$\tilde{W}_{xx}(t, f) = M(t, f) W_{xx}(t, f), \quad (11)$$

which satisfies, for all t and f , the following conditions

$$\tilde{W}_{xx}(t, f) \approx W_{jj}(t, f) \quad (12)$$

$$\tilde{W}_{xx}(t, f) \cdot W_{pp}(t, f) \approx 0, \quad (13)$$

provided that the jammers do not occupy significant space in the t-f plane.

3.3. Selection of the Threshold Value

It is important to determine a threshold value such that the resulting mask satisfies (12) and (13). To this end, the properties of $2\text{Re}(W_{jw}(t, f))$ and $W_{ww}(t, f)$ are examined

in light of the fact that the input SNR of a GPS signal is much below 0 dB. These properties have been generally discussed, for example, in [7]. In this paper, discussion is limited to the simple situations where the noise is Gaussian and white, and the TFD is Wigner or EDTWD. In this case, it is easy to confirm that $2\text{Re}(W_{jw}(t, f))$ is a zero-mean Gaussian random process with

$$\begin{aligned} & \text{var}(2\text{Re}(W_{jw}(t, f))) \\ &= E[(W_{jw}(t, f) + W_{jw}^*(t, f))(W_{jw}(t, f) + W_{jw}^*(t, f))^*] \\ &= E[W_{jw}(t, f)W_{jw}^*(t, f)] + E[W_{jw}^*(t, f)W_{jw}^*(t, f)] \\ &\quad + E[W_{jw}^*(t, f)W_{jw}(t, f)] + E[W_{jw}^*(t, f)W_{jw}(t, f)], \end{aligned} \quad (14)$$

where $E[\cdot]$ denotes the expected value operator. By using the noise properties, it is clear that the first two terms in the right side of (14) result in 0. Under the zero mean Gaussian assumption of the noise,

$$\begin{aligned} & \text{var}(2\text{Re}(W_{jw}(t, f))) = 2E[W_{jw}(t, f)W_{jw}^*(t, f)] \\ &= 2 \sum_{k_1:t+\frac{k_1}{2} \in Z} \sum_{k_2:t+\frac{k_2}{2} \in Z} E \left[j(t + \frac{k_1}{2})j^*(t + \frac{k_2}{2}) \right. \\ &\quad \left. \cdot w(t - \frac{k_2}{2})w^*(t - \frac{k_1}{2})e^{-j2\pi(k_1-k_2)f} \right] \\ &= 2\sigma \sum_{k:t+\frac{k}{2} \in Z} j(t + \frac{k}{2})j^*(t + \frac{k}{2}) \\ &= 2\sigma \sum_{l=1}^L |j(l)|^2 = 2\sigma P_j, \end{aligned} \quad (15)$$

where $P_j = \sum_{l=1}^L |j(l)|^2$ is the total energy of the jammer over the L samples. Equation (15) reveals that the variance of the crossterm between the jammer and noise is constant, independent of t and f . Since $P_j \approx P_x$, which can be estimated from the received signal, and σ is usually known for a given receiver, the crossterm variance can be estimated without difficulty.

Therefore, to avoid the crossterm between the jammer and noise in the masked t-f region, the threshold value is set proportional to the standard deviation of the crossterm as

$$C = \alpha\sqrt{\sigma P_x}, \quad (16)$$

where α is a constant. By considering the Gaussian random nature of the crossterm $2\text{Re}(W_{jw}(t, f))$, α can be chosen as about 3 to 5. Numerical results to examine the effect of α are given in Section 5.

Another important parameter to consider in the determination of the threshold value is the jammer autoterm $W_{jj}(t, f)$ — the threshold value should be smaller than $W_{jj}(t, f)$ over most of its mainlobe t-f region. With reasonably long block length and highly localized t-f signature of the jammer, however, the above threshold value usually satisfies this requirement.

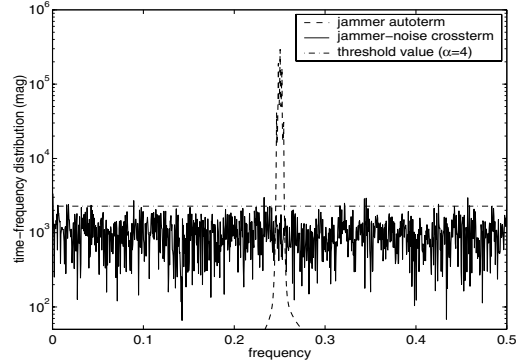


Fig. 1 Jammer autoterm, jammer-noise crossterm, and the threshold value.

Fig. 1 shows the EDTWDs for the jammer autoterm W_{jj} and jammer-noise crossterm $2\text{Re}(W_{jw}(t, f))$ at $t = 512$. The jammer is an AM-FM signal, where the normalized start and end frequency are 0.15 and 0.35, respectively, and the AM modulation factor is 0.8. The input SNR in this figure is -16 dB and the input jammer-to-noise ratio (JNR) is 25 dB. The threshold value with $\alpha = 4$ is also shown in dashed line.

3.4. Multiple Jammer Consideration

When multiple jammers arrive at the receiver, t-f synthesis may still prove effective, provided that each jammer is distinguishable in the t-f domain. In this situation, each jammer is individually synthesized from the t-f domain and subtracted from the received signal.

It is maintained that, in multiple jammer situations, the threshold value obtained from (16) remains valid. In this case, however, the crossterms between the jammers and the noise should be all considered in (15), and $P_x \approx \sum_{v=1}^J P_{j,v}$.

It is worth noting that crossterms between jammers often have high value, and the selection of only the jammer autoterm may become difficult. In this case, the use of multiple array sensors can help to reduce the crossterms and reinforce the jammer autoterm. Multi-sensor application is discussed in Section 4.

3.5. Jammer Mitigation

After the mask $M_v(t, f)$ is determined, and the jammer waveform $\tilde{j}_v(t)$ is synthesized with phase ambiguity from the masked TFD $\tilde{W}_{jj,v}(t, f)$, we construct the jammer subspace. For this purpose, instead of $\tilde{j}_v(t)$, we rather use the unit-norm eigenvector \mathbf{u}_v defined in (8) for $v = 1, \dots, J$. The synthesized waveform of the v th jammer with correct phase information is expressed as

$$\hat{\mathbf{j}}_v = \mathbf{u}_v \mathbf{u}_v^H \mathbf{x}. \quad (17)$$

The jammer-suppressed signal vector can then be expressed

as

$$\mathbf{x}^\perp = \mathbf{x} - \sum_{v=1}^J \hat{\mathbf{j}}_v = (\mathbf{I} - \mathbf{U}\mathbf{U}^H) \mathbf{x}, \quad (18)$$

where \mathbf{I} is the identity matrix, and $\mathbf{U} = [\mathbf{u}_1, \dots, \mathbf{u}_J]$.

4. MULTI-SENSOR ARRAY CONSIDERATION

In this section, we consider the use of multiple array sensors in the underlying anti-jamming problem. Compared with the single antenna application, the use of multiple array sensors may further improve the performance in terms of signal enhancement and jammer cancellation. The use of multiple antennas can improve the performance in two ways: (a) For multiple array sensor situations, averaged time-frequency distributions can be exploited to reduce the effect of crossterms as well as noise. (b) The use of array sensors extends the dimension and therefore can reduce the signal distortion due to orthogonal projection. Before we discuss these features, we first discuss the concept of array averaged TFD [8].

4.1. Array Averaged Time-Frequency Distributions

For notation simplicity, we consider a general case and let $y_m(t)$ represent the received signal at the m th array sensor ($m = 1, \dots, M$), and $s_k(t)$ the K source signals ($k = 1, \dots, K$). $y_m(t)$ and $s_k(t)$ are related by

$$y_m(t) = a_{k,m} s_k(t), \quad (19)$$

where $\mathbf{a}_k = [a_{k,1}, \dots, a_{k,M}]^T$ forms the spatial signature of the k th signal. The spatial signature for different signals are considered linearly independent, each is normalized to norm M . We can express the TFD of the signal at the m th sensor $y_m(t)$ as

$$W_{y_m y_m}(t, f) = \sum_{k_1=1}^K \sum_{k_2=1}^K a_{k_1, m} a_{k_2, m}^* W_{s_{k_1} s_{k_2}}(t, f). \quad (20)$$

Averaging $W_{y_m y_m}(t, f)$ over the array yields

$$\begin{aligned} \bar{W}_{yy}(t, f) &= \frac{1}{M} \sum_{m=1}^M W_{y_m y_m}(t, f) \\ &= \sum_{k_1=1}^K \sum_{k_2=1}^K \left(\frac{1}{M} \mathbf{a}_{k_2}^H \mathbf{a}_{k_1} \right) W_{s_{k_1} s_{k_2}}(t, f) \quad (21) \\ &= \sum_{k_1=1}^K \sum_{k_2=1}^K \beta_{k_1 k_2} W_{s_{k_1} s_{k_2}}(t, f) \end{aligned}$$

where the following spatial correlation coefficient is defined

$$\beta_{k_1 k_2} = \frac{1}{M} \mathbf{a}_{k_2}^H \mathbf{a}_{k_1}. \quad (22)$$

Equation (21) shows that $\bar{W}_{yy}(t, f)$ is a linear combination of the auto-source and cross-source TFDs, weighted by the respective spatial correlation coefficients. Since

$$|\beta_{k_1 k_2}| < 1, k_1 \neq k_2 \text{ and } \beta_{k_1 k_2} = 1, k_1 = k_2, \quad (23)$$

the multiplication constants in (22) associated with the auto-source TFDs are always greater than those for the cross-source TFDs. This property is the key offering of the array averaging TFDs and is shown to improve the signal synthesis performance.

Theoretically, the spatial correlation coefficient between two different signals can always be reduced to a small value with the use of large number of array sensors. Specifically, when all spatial signatures are orthogonal, i.e., $\beta_{k_1 k_2} = 0$ for any $k_1 \neq k_2$, all source signal crossterms are entirely eliminated and only the autoterms are maintained, which is most desirable from the signal synthesis perspective.

4.2. Impact in Mask Construction

Herein, we consider the impact of using array averaged TFDs on the crossterms between different jammers as well as the crossterms between the jammers and the noise. The array averaging reduces the crossterms between jammers. The significance of the reduction is determined by the jammer spatial correlations. Further, under the spatial white noise assumption, the covariance of the crossterm between a jammer and the noise is reduced by the factor of M . It is easy to confirm that

$$\begin{aligned} \text{var} [\bar{W}_{j_v w}] &= \text{var} \left[\frac{1}{M} \sum_{m=1}^M W_{j_{v,m} w_m} \right] \\ &= \frac{1}{M^2} \sum_{m=1}^M \text{var} [W_{j_{v,m} w_m}] = \frac{2\sigma}{M} \bar{P}_{j,v}. \end{aligned} \quad (24)$$

Therefore, the threshold value for the M sensor case becomes

$$C = \alpha \sqrt{\sigma \bar{P}_x / M}. \quad (25)$$

Note that in (24) and (25), $\bar{P}_{j,v}$ and \bar{P}_x are, respectively, the energy of the v th jammer and the signal arrival averaged over the M antennas.

4.3. Disjoint and Joint Space-Time Processing

Upon estimating the jammer signatures using the array averaged TFD, different approaches can be implemented to mitigate the jammers. In the disjoint space-time processing (STP) method, the jammer is removed from each sensor data by projecting the respective received signal into the orthogonal subspace, as described in (18). The jammer subspace is the same for all sensors. The jammer-free GPS signal is then combined in the sense of maximum ratio diversity by using the matched weight vector. Another approach is to first estimate the spatial signature of each jammer and construct the respective joint spatio-temporal signature. Then, the received signal spatio-temporal vector is projected onto the subspace orthogonal to the jammers' joint space-time signatures. Denote \mathbf{x}_m as the received signal vector at the m th sensor, and let $\mathbf{X} = [\mathbf{x}_1^T, \dots, \mathbf{x}_M^T]^T$. The spatial signature of the v th jammer, \mathbf{a}_v , is estimated by using the

maximum likelihood estimator

$$\hat{\mathbf{a}}_v = \sqrt{M} \mathbf{u}_v^H \mathbf{X} / \|\mathbf{u}_v^H \mathbf{X}\|. \quad (26)$$

The performance comparison of these two approaches is discussed in detail in [2]. While using multiple sensors at disjoint STP provides the array gain to improve the output SNR, the joint STP shows additional performance improvement because of increased dimensionality of the signal relative to the jammer.

5. COMPUTATION RESULTS

Simulation examples are used to demonstrate the effectiveness of the proposed method and to examine the impact of the mask selectivity. We consider the case where an AM-FM jammer impinges on the receiver along with a GPS signal. The AM-FM jammer's start and end frequency are 0.15 and 0.35, respectively, and the AM modulation factor is 0.8. The input SNR of the GPS signal is -16 dB, and the input JNR is 25 dB. The block size L is 256 and the variance used in evaluating the output SINR is obtained based on 200 independent trials for the GPS signal from each satellite. The output SINR results are then averaged over the GPS signals from different satellites.

Fig. 2 shows the output SINR performance in a solid line versus the value of α . The dashed line shows the output SINR upper bound obtained using the true jammer signature, or subspace. From the solid line of this figure, the dependence of the output SINR on the value of α is evident. A small α results in GPS signal reduction, whereas a large α results in insufficient jammer excision. The output SINR shows large output values when α is between 2 and 9, at which the output SINR is very close to the upper bound.

Fig. 3 shows the output SINR performance where two antennas are used at the receiver. The DOAs of the GPS signal and jammer are, respectively, 20° and -20° . It is evident from this figure that, compared with the single antenna case, that the SINR improvement is more than the 3dB array gain. This is because of the improved jammer estimation and spatial selectivity available for the array processing techniques.

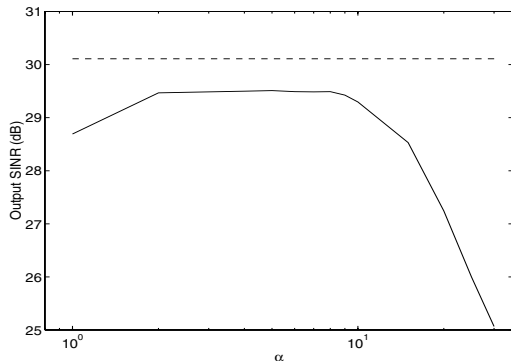


Fig. 2 Output SINR vs. α (1 antenna case).

6. CONCLUSION

A nonstationary jammer suppression technique for GPS receivers, based on time-frequency distributions (TFDs), is proposed. The effect of the t-f mask in capturing the jammer power is discussed. The selection of the mask threshold value has been investigated. We have also considered array processing techniques in the underlying problem, and the advantages have been demonstrated in terms of array gain, improved jammer estimation, and spatial selectivity.

REFERENCES

- [1] L. Zhao, M. G. Amin, A. R. Lindsey, and Y. Zhang, "Subspace projection array processing of FM jammer in GPS receivers," in *Proc. 34th Annual Asilomar Conference on Signals, Systems, and Computers*, Pacific Grove, CA, Nov. 2000.
- [2] Y. Zhang and M. G. Amin, "Array processing for non-stationary interference suppression in DS/SS communications using subspace projection techniques," submitted to *IEEE Trans. Signal Processing*.
- [3] G. Boudreaux-Bartels and T. Parks, "Time-varying filtering and signal estimation using Wigner distribution synthesis techniques," *IEEE Trans. ASSP*, vol. 34, pp. 442–451, June 1986.
- [4] F. Hlawatsch and W. Kozek, "Time-frequency projection filters and time-frequency signal expansions," *IEEE Trans. Signal Processing*, vol. 42, pp. 3321–3334, Dec. 1994.
- [5] F. Hlawatsch and W. Krattenthaler, "Bilinear signal synthesis," *IEEE Trans. ASSP*, vol. 40, pp. 352–363, Feb. 1992.
- [6] J. Jeong and W. Williams, "Time-varying filtering and signal synthesis," in *Time-Frequency Signal Analysis — Methods and Applications*, B. Boashash ed., Longman Cheshire, 1995.
- [7] L. J. Stankovic and S. Stankovic, "Wigner distribution of noisy signals," *IEEE Trans. Signal Processing*, vol. 41, pp. 956–960, Feb. 1993.
- [8] W. Mu, Y. Zhang, and M. G. Amin, "Bilinear signal synthesis in array processing," in *Proc. ICASSP*, Salt Lake, UT, May 2001.

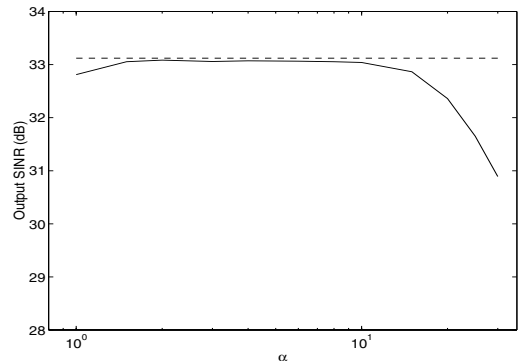


Fig. 3 Output SINR vs. α (2 antenna case).